Circuit Modeling and Simulation of Integrated Microfluidic Systems

Aveek N. Chatterjee* and N. R. Aluru**
Beckman Institute for Advanced science and Technology - University of Illinois, Urbana-Champaign
*Doctoral student, University of Illinois at Urbana-Champaign
** Corresponding Author, Associate Professor, University of Illinois at Urbana-Champaign, e-mail: aluru@uiuc.edu, http://www.staff.uiuc.edu/~aluru.

ABSTRACT

A combined circuit-device model for the analysis of integrated microfluidic system is presented. The complete model of an integrated microfluidic device incorporates modeling of the fluidic transport, chemical reaction, reagent mixing and separation. The microfluidic flow can be caused by an applied electrical potential gradient and/or a pressure gradient. In the proposed compact model, the fluidic network has been modeled by a circuit based representation and the other modules of the μ-TAS have been represented by a device model. As an example, we present the modeling and simulation of a lab-on-a-chip.

Keywords: microfluidics, lab-on-a-chip, circuit-modeling, simulation

1 INTRODUCTION

In this paper, we report on the advancement of a compact model for micro/nanofluidic transport driven by a combined electric field and pressure gradient, which had been introduced earlier by Qiao et. al.[1]. The new model has incorporated a number of additional elements, which were not included in the simple model that was proposed earlier (e.g. inclusion of capacitive elements, complete circuit representation of fluidic transport, circuit model for non-slip flow etc.). In addition, the new model is able to simulate mixing, reaction and separation, which are some of the most important functions of an integrated μ-fluidic system. Finally, an example is considered, where the combined circuit-device model has been demonstrated successfully.

2 MODEL DEVELOPMENT

The derivation of the circuit model for a flow driven by combined pressure gradient and electrical potential gradient is described in the beginning of this section. The compact model for the fluidic transport is composed of two parts, namely, the electrical part and the fluidic part.

2.1 Electrical Model

For microfluidic devices that rely on electrokinetic force as the driving force, the electric field must be solved first. In the case of electroosmotic flow, the potential field due to an applied potential can be computed by solving the Laplace equation [2]. Therefore, the axial potential variation can be represented by linear electrical resistances [1]. The EDL can be decomposed into the stern layer and the diffuse layer [3]. As the stern layer and the diffuse layer store charge, the capacitance associated with these layers is important. Figure 1 and 2 illustrate a typical cross shaped channel segment in a microfluidic system and its circuit representation, respectively. The expression for computing the electrical resistance of a solution filled channel is given in [1]. The expression for the effective capacitance is given by:

$$\left(C_{eff,i}\right)^{-1} = \left(C_{st,i}\right)^{-1} + \left(C_{dl,i}\right)^{-1} \tag{1}$$

where, $C_{st,i}$ is the capacitance of the stern layer of the i^{th} channel (shown in figure 2), $C_{dl,i}$ is the capacitance of the diffuse layer of the i^{th} channel and $C_{eff,i}$ is the effective capacitance of the i^{th} channel. The expression for C_{st} and C_{dl} are given in [3] and [4], respectively. Using the relation between capacitance of a layer and the charge stored in a layer we get the following expression:

$$C_{eff,i}\psi_{0,i} = q_{st,i} = \sigma_{T,i}A_{s,i} \tag{2}$$

or

$$\psi_{0,i} = \frac{\sigma_{T,i}A_{s,i}}{C_{eff,i}} \tag{3}$$

where $\psi_{0,i}$ is the surface potential on the i^{th} channel and $q_{st,i}$ is the total charge stored in the EDL of the channel. From the principle of conservation of charge it can be shown that the net charge stored in the EDL neutralizes the total surface charge.

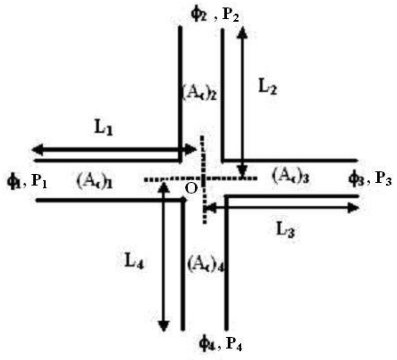

Figure 1: A typical cross-shape channel segment of a microfluidic system. The electrical potentials, $\phi_{1\text{-}4}$, and pressures, $P_{1\text{-}4}$, are given.

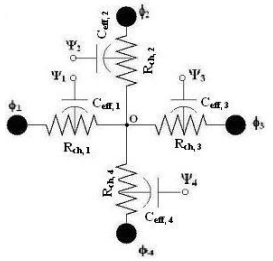

Figure 2: The electrical network representation for the electrical part. $R_{ch,1\text{-}4}$ are the electrical resistances, $\Psi_{1\text{-}4}$ are the surface potentials of the channel walls and $C_{eff,1\text{-}4}$ are the capacitances of the EDLs.

2.2 Fluidic Model

For the fluidic transport driven by an electrical field and/or a pressure gradient, the "through quantities" are the flow rates through the channels and the "across quantities" are the electrical potential differences and the pressure differences imposed on the fluidic channels. In this section we present a derivation of the constitutive equation relating the "through quantities" to the "across quantities".

In those cases, where the thickness of the EDL is insignificant compared to the depth or diameter of the channel the effect of the electrokinetic force can be represented by a slip velocity at the wall given by the Helmholtz-Smoluchowski equation [1]. The slip velocity is a function of the ζ potential of the channel wall [2] and the ζ potential can be related to the surface potential of the channel wall [5] through the Debye-Huckel theory. The capacitance model described in section 2.1 can be used for computing the surface potential of the channel wall. The velocity profile across a capillary slit is a function of only the slip velocity and the pressure gradient [1], i.e.,

$$u = -\frac{1}{2\mu}\frac{dp}{dx}\left(y^2 - \frac{h^2}{4}\right) + u_{slip} \tag{4}$$

where x denotes the stream direction of the channel, y denotes the transverse direction across the channel and h is the channel depth. In the region where the flow is fully developed, it can be shown [1] that the pressure calculation is reduced to Laplace equation. Integrating the velocity profile given in equation (4) across the cross-section of the capillary slit, we get the following expression for the flow rate per unit width:

$$Q = \left(\frac{h^3}{12\mu L}\right)\Delta p + \left(\frac{\varepsilon\varsigma}{\mu L}h\right)\Delta\phi \tag{5}$$

For the i^{th} channel in an array of channels, equation (5) can be represented as:

$$Q_i = H_i \Delta p_i + E_i \Delta\phi_i \tag{6}$$

where H_i is the hydraulic conductance of the i^{th} channel and E_i is the electro-hydraulic conductance of the i^{th} channel. The expressions for H_i and E_i for the capillary slit are given in equation (5).

The slip velocity model discussed above can be employed when the Debye length is thin compared to the channel width. However, when the Debye length is comparable to the channel width, (typically, for channels smaller than 100 nm) the slip velocity model may not be accurate. For a rectangular channel or a capillary slit, the velocity profile is given by the following expression [5]:

$$u_{(y)} = -\frac{1}{2\mu}\frac{dp}{dx}\left(y^2 - \frac{h^2}{4}\right) - \frac{\varepsilon}{\mu}\nabla\phi\left(\psi_0 - \psi_{(y)}\right) \tag{7}$$

where

$$\psi_{(y)} = \frac{\psi_0 \cosh\left(y/\lambda_D\right)}{\cosh\left(h/\lambda_D\right)} \tag{8}$$

Integrating the velocity profile given in equation (7) across the cross section and using equation (8), we get the following expressions for the hydraulic conductance and the electro-hydraulic conductance of the i^{th} channel:

$$H_i = \frac{h_i^3}{12\mu_i L_i} \tag{9}$$

$$E_i = \frac{\varepsilon_i}{\mu_i L_i}\psi_0\left(2h_i - 2\lambda_D\frac{\sinh\left(h/\lambda_D\right)}{\cosh\left(h/\lambda_D\right)}\right) \tag{10}$$

where λ_D is the Debye length [5].

Figure 3 shows the circuit representations of the fluidic domain for the cross-shaped channel segment shown in figure 1. It is to be noted that the total flow is the sum of the electrokinetically driven flow and the pressure driven flow. In the case of channels with integrated elastic parts (e.g. a flexible membrane), a capacitive element needs to be included in the circuit model of the fluidic domain as shown in figure 3. The fluidic capacitor can be modeled as:

$$C_{fl} = \frac{\iint_{\Gamma} w(x,y)\,d\Gamma}{p} \tag{11}$$

where C_{fl} is the fluidic capacitance, w is the deflection, Γ is the total surface area of the flexible membrane and p is the pressure.

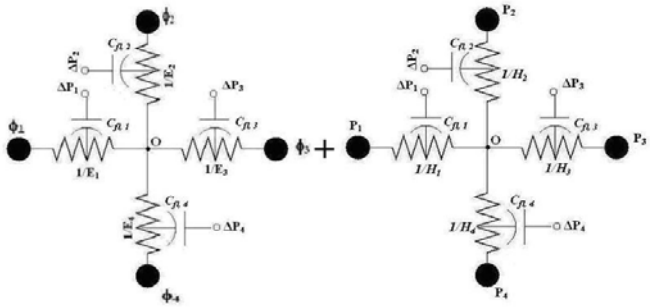

Figure 3: Circuit representation of the electrokinetically driven flow is on the left and circuit representation of the pressure driven flow is given on the right. The "plus" sign between the two figures indicates that the total flow is the superimposition of the electrokinetically driven flow and the pressure driven flow.

2.3 Device Model: Reactions

Consider a scheme in which the chemical species A and B are transported to the reaction chamber, where they undergo a second order reversible reaction process to produce specie C. The governing equations for this reaction process are given by [6]:

$$\frac{\partial m_A}{\partial t} = Q_A C_A - k_1(m_A)(m_B) + k_2(m_C) \quad (12)$$

$$\frac{\partial m_B}{\partial t} = Q_B C_B - k_1(m_A)(m_B) + k_2(m_C) \quad (13)$$

$$\frac{\partial m_C}{\partial t} = k_1(m_A)(m_B) - k_2(m_C) \quad (14)$$

where Q_i is the flow rate of the i^{th} specie, which is computed from the fluidic transport model (or known from the design specifications), C_i is the concentration of the i^{th} specie, m_i is the number of moles of the i^{th} specie present in the reaction chamber, k_1 is the forward reaction rate and k_2 is the backward reaction rate. Trapezoidal method is used to discretize the ODEs given in equations (12) to (14). The non-linear discretized equations are then solved by employing the Newton-Raphson scheme.

2.4 Device Model: Separation

Consider an example, where two species *A* and *B* are to be separated using the separation channel. Assume that, specie *A* is unit-positively charged and specie *B* is unit negatively charged, while the surface of the channel has a negative fixed charge. In this case, the electro-osmotic flow through the channel would be from the anode side to the cathode side. The electrophoretic flow for *A* would be from anode to cathode but that for *B* it would be in the opposite direction. This is due to the difference in the electrophoretic velocity of these two species. Thus, the ratio of the rate of molar increment at the outlet of the separation channel for the two species is given by the following expression:

$$Separation\ \ Ratio = \frac{\left(Q_{os} + sign(z_A) \times \left|Q_{ph}\right|_A\right) c_A^{in}}{\left(Q_{os} + sign(z_B) \times \left|Q_{ph}\right|_B\right) c_B^{in}} \quad (15)$$

where, c_A^{in} is the concentration of specie A at the inlet, c_B^{in} is the concentration of specie B at the inlet and Q_{os} is the bulk flow, which is computed from equation (6). The electrophoretic flux can be represented by a circuit model [6]:

$$\left|Q_{ph}\right|_i = \left(\frac{FD_i|z|_i}{RT}\frac{A_c}{L}\right)\Delta\phi = \Im_i \Delta\phi \quad (16)$$

Where, $\Im_i$ is the electrophoretic flux conductance of the i^{th} specie in the separation channel.

3 RESULTS

As an example, we consider a lab-on-a-chip system (figure 4), which is designed based on the "Nanochip" reported by Becker et. al.[4]. The various chemical species are transported to the different modules on the chip from their sources by using electrokinetic transport. One third of the channels (marked as set A1 in figure 4) perform the dual role of fluid transport and passive mixing. These channels have been designed in such a way that the characteristic dimension at a given level is half of that at the previous level. Thus, the homogeneity of the sample being transported increases. Figure 5 shows the dependence of the homogeneity of the mixture [7], e_{mix}, on the number of split levels [6]. Electrophoretic separation and electrokinetic transport is the governing mechanism through the set of channels marked as A2 (in figure 4), while electrokinetic transport is the governing mechanism through the set of channels marked as A3. The specie in set A1 (say A) is then transported to the detection module (D), where it reacts with specie B (already present in the detection chamber) to produce specie C, which can be used for off-chip detection. Figure 6 shows the variation in the rate of formation of specie C with time for different applied potentials. The chemical species (G and H) transported through the channels A2 and A3 are transported to the reactor module (R in figure 4), where they undergo a second order reversible chemical reaction to produce another chemical specie, F. Figure 7 shows the effect of the number of input ports on the variation of the concentration of F with time.

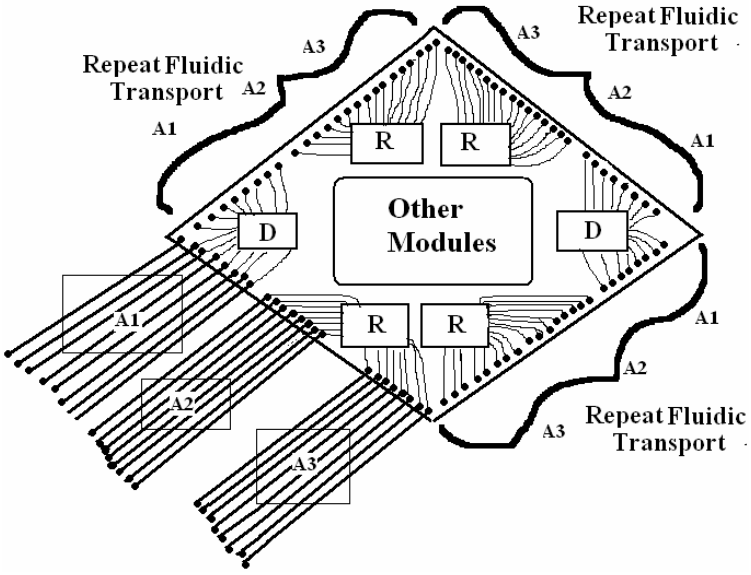

Figure 4: The schematics of the microfluidic chip considered as an example. The fluidic transport system represented on the south-west side of the chip is duplicated on the other sides.

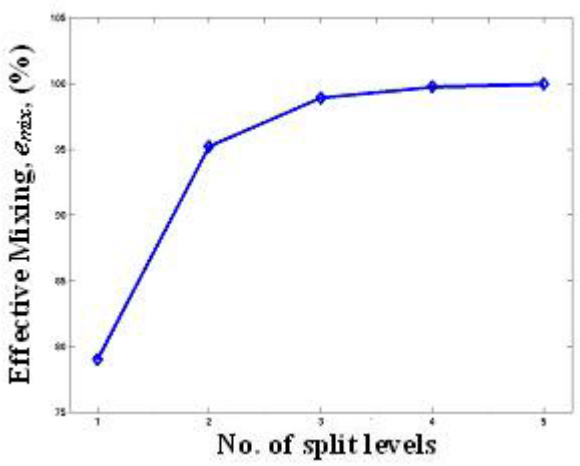

Figure 5: The dependence of the effectiveness of the mixing (i.e. homogeneity of the mixture) on the number of split levels used.

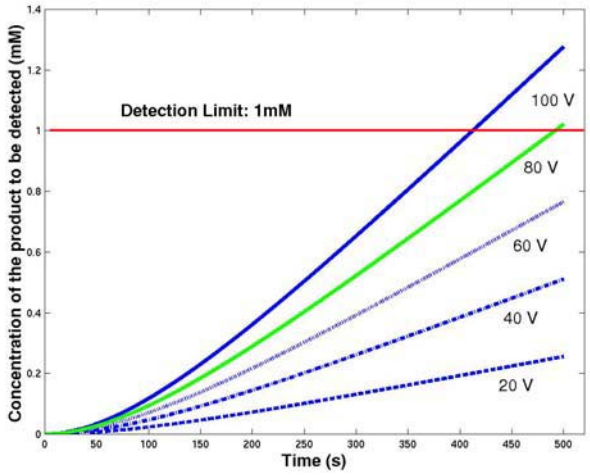

Figure 6: Concentration (C) versus time for various applied potentials.

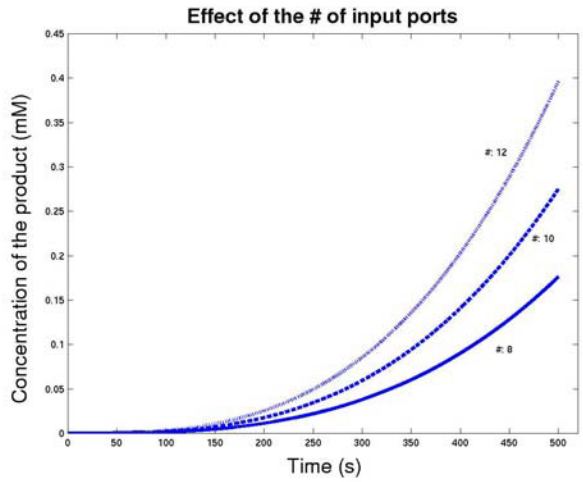

Figure 7: Concentration (F) versus time for different numbers of input ports per side of the microfluidic chip.

4 CONCLUSION

An advanced compact model for rapid analysis of microfluidic systems is presented. The fluidic transport system is represented by an electrical circuit network. Therefore, the fluidic variables (e.g. flow rate, pressure etc.) can be computed using the same schemes, which are used for computing the electrical variables. The new circuit model is significantly self sufficient and considers a number of additional elements compared to the compact model presented by Qiao et. al.[1]. As a result the circuit model presented in this paper can capture the physics of the fluidic transport process in much greater detail. Device models of the significant modules of a μ-TAS have also been presented in this paper. The integration of the circuit model for the fluidic transport system and the device models for the modules of the lab-on-a-chip example has been demonstrated. In conclusion, the circuit model based microfluidic-CAD tool presented here can be used to simulate and design next generation very large scale integrated (VLSI) microfluidic chips.

REFERENCES

1. R. Qiao and N. R. Aluru, "A compact model for electroosmotic flows in microfluidic devices", *J. Micromech. Microeng.*, Vol. **12**, pp. 625-635, 2002.
2. M. Mitchell, R. Qiao and N. R. Aluru, "Meshless analysis of steady state electroosmotic transport", *J. Microelectromech. Syst.*, Vol. **9**, pp. 435-449, 2000.
3. K. B. Oldham and J. C. Myland, *Fundamentals of Electrochemical Science*, Academic Press Inc: San Diego, 1994.
4. H. Becker and L. E. Locascio, "Polymer microfluidic devices", *Talanta*, Vol. **56**, pp. 267-287, 2002.
5. N. A. Patankar and H. H. Hu, "Numerical simulation of electroosmotic flow", *Anal. Chem.*, Vol. **70**, pp. 1870-1881, 1998.
6. A. N. Chatterjee and N. R. Aluru, "Combined circuit/device modeling and simulation of integrated microfluidic systems", *to be submitted for Journal Publication*.
7. P. Huang and K. S. Breuer, "Performance and scaling of an electro-osmotic mixer", *The 12th International Conference on Solid-State Sensors, Actuators and Microsystems (Transducers 2003, Boston)*, pp. 663-666, 2003.
8. S. C. Jacobson, T. E. McKnight and J. M. Ramsey, "Microfluidic devices for electrokinetically driven parallel and serial mixing", *Anal. Chem.*, Vol. **71**, pp. 455-4459, 1999.